Developmental Biology **240,** 499–516 (2001)
doi:10.1006/dbio.2001.0481, available online at http://www.idealibrary.com on IDEAL®

Smad7 Misexpression during Embryonic Angiogenesis Causes Vascular Dilation and Malformations Independently of Vascular Smooth Muscle Cell Function

Neil Vargesson and Ed Laufer[1]

Department of Genetics and Development, College of Physicians and Surgeons, Columbia University, 701 West 168th Street, New York, New York 10032

Numerous *in vitro* and *in vivo* studies implicate transforming growth factor-β (TGFβ) superfamily signaling in vascular development and maintenance. Mice and humans with mutations in TGFβ superfamily signaling pathway genes exhibit a range of vascular defects that include dilated, fragile and hemorrhagic vessels, defective angiogenic remodeling, severe vascular malformations including arterio-venous malformations, and disrupted vascular smooth muscle cell recruitment and maintenance. Despite a wealth of data, the functions of TGFβ superfamily signals during angiogenesis are poorly defined, since early embryonic lethality and difficulty distinguishing between primary and secondary defects frequently confound phenotypic interpretation. To perturb TGFβ superfamily signaling during angiogenesis, we have misexpressed Smad7, an intracellular antagonist of TGFβ superfamily signaling, in the developing chick limb and head. We find that the great vessels are strikingly dilated and frequently develop intra and intervascular shunts. Neither noggin nor dominant negative BMP receptor misexpression causes similar vascular phenotypes. However, simultaneous misexpression of constitutively active BMP receptors with Smad7 suppresses the Smad7-induced phenotype, suggesting that a BMP-like intracellular pathway is the target of Smad7 action. Despite the gross morphological defects, further analyses find no evidence of hemorrhage and vessel structure is normal. Furthermore, enlarged vessels and vascular malformations form in either the presence or absence of vascular smooth muscle, and vascular smooth muscle cell recruitment is unperturbed. Our data define the TGFβ superfamily pathway as an integral regulator of vessel caliber that is also essential for appropriate vessel connectivity. They demonstrate that dilation need not result in vessel rupture or hemorrhage, and dissociate vessel maintenance from the presence of a vascular smooth muscle cell coat. Furthermore they uncouple vascular smooth muscle cell recruitment and differentiation from TGFβ superfamily signaling.

Key Words: **TGFβ signaling; Smad7; arterio-venous malformation; vascular smooth muscle; endothelial cell; artery; vein; vessel caliber; angiogenesis; vasculogenesis; vasculature.**

INTRODUCTION

The vascular network of the embryo, and ultimately of the adult, originates in early embryonic development from a small population of mesodermal endothelial precursor cells. During vasculogenesis, endothelial cell precursors coalesce to form a capillary plexus that is subsequently remodeled as vessels enlarge, as arterial-venous distinctions are established and as mural cells, such as capillary-associated pericytes and vascular smooth muscle cells (VSMC), are recruited. Later, during angiogenesis, new vessels are generated from existing ones and are similarly remodeled (Daniel and Abrahamson, 2000; Hungerford and Little, 1999; Risau, 1997; Yancopoulos *et al.*, 2000). These processes are molecularly distinguishable as angiogenesis requires intercellular signals, such as the angiopoietins and their receptors, that appear to be dispensable for normal vasculogenesis (Gale and Yancopoulos, 1999; Puri *et al.*, 1995; Sato *et al.*, 1995; Suri *et al.*, 1996; Vikkula *et al.*, 1996; Yancopoulos *et al.*, 2000). During development the vessels of the developing head, body and extraembryonic regions

[1] To whom correspondence should be addressed. Fax: 1-212-923-2090. E-mail: elaufer@columbia.edu.

0012-1606/01 $35.00

form via vasculogenesis and subsequently are elaborated by angiogenesis. The developing limb is predominantly vascularized by angiogenesis, as new vessels sprout from pre-existing flank vessels and invade the nascent limb bud (Ambler *et al.*, 2001; Brand-Saberi *et al.*, 1995; Coffin and Poole, 1988; Daniel and Abrahamson, 2000; Pardanaud *et al.*, 1987; Pardanaud *et al.*, 1989; Poole and Coffin, 1989; Risau, 1997).

TGFβ superfamily ligands of the TGFβ, activin, and bone morphogenetic protein (BMP) families stimulate heteromeric serine/threonine kinase receptors to activate Smad protein-mediated intracellular signal transduction. Phosphorylated positive Smad proteins hetero-oligomerize with a common partner, Smad4, translocate to the nucleus and regulate target gene expression (Massague, 1998; Massague and Chen, 2000; Miyazono, 2000). Specificity is imparted through differential ligand binding by the receptors, and subsequently activation of pathway-specific positive Smads. Thus, for example, BMPs activate two signaling receptors, BMPR Ia and BMPR Ib (Alk3 and Alk6), that in turn activate Smad1, Smad5 and Smad8, but not Smad2 or Smad3, which are regulated by TGFβ and activin ligands and their cognate receptors (Eppert *et al.*, 1996; Hoodless *et al.*, 1996; Massague and Chen, 2000).

Multiple TGFβ superfamily ligands, receptors and signaling proteins are expressed in association with the developing vasculature and have multiple functions during vascular development (Gatherer *et al.*, 1990; Pelton *et al.*, 1989; Pelton *et al.*, 1990; Roberts and Sporn, 1992; Schmid *et al.*, 1991). *In vitro* studies suggest that TGFβ influences endothelial cell growth, regulates extracellular matrix deposition, modulates endothelial cell migration and fusion into capillary tubes, and controls vessel lumen size (Gajdusek *et al.*, 1993; Madri *et al.*, 1988; Merwin *et al.*, 1990; Pepper *et al.*, 1990; Pepper *et al.*, 1993; Pepper, 1997; Roberts and Sporn, 1989). However, the nature of the endothelial cell response to added TGFβ ligand can vary dramatically depending on experimental design, thus making specific functional assignments difficult (Daniel and Abrahamson, 2000; Klagsbrun and D'Amore, 1991).

Recent studies have focused on *in vivo* loss of function analyses to define roles of this pathway in vascular development. Loss of individual signaling components can lead to severe vascular defects resulting in embryonic lethality either during initial vasculogenesis, or in the early stages of angiogenic remodeling (Dickson *et al.*, 1995; Oshima *et al.*, 1996; Lawler *et al.*, 1998; Pepper, 1997). Activin receptor-like kinase 1 (Alk1), a TGFβ and activin-binding receptor, endoglin (Eng), a TGFβ superfamily coreceptor and Smad5 are three such genes that are required for normal angiogenesis. Vessels in Alk1, Eng or Smad5 null mutant animals are fragile, hemorrhagic and dilated. Expression levels of extracellular matrix remodeling enzymes are abnormal, and recruitment of vascular smooth muscle cells (VSMC) to the vascular endothelium is defective (Chang *et al.*, 1999; Li *et al.*, 1999; Oh *et al.*, 2000; Pepper, 1997; Urness *et al.*, 2000; Yang *et al.*, 1999). In addition Alk1-deficient mice develop arteriovenous malformations (AVMs) that are characterized by shunting between the arterial and venous circulations, and an inability to establish molecular and morphological distinctions between arteries and veins (Urness *et al.*, 2000). These phenotypes resemble those observed in human patients suffering from hereditary hemorrhagic telangiectasia (HHT), a life-threatening condition linked to haploinsufficiency of ALK1 or ENG (Shovlin and Letarte, 1999).

Emerging models suggest that primary vascular functions of TGFβ signaling are to promote VSMC recruitment and subsequently VSMC differentiation, and to inhibit endothelial proliferation via VSMC-endothelial interactions. However, both TGFβ superfamily and non-TGFβ superfamily (e.g., angiopoietins) signaling mutants have disrupted VSMC-endothelial interactions that are consistently associated with vessel dilation, fragility and hemorrhage (Puri *et al.*, 1995; Sato *et al.*, 1995; Suri *et al.*, 1996; Vikkula *et al.*, 1996). Thus, it is not clear if the direct consequences of reduced TGFβ signaling are loss of VSMCs, vessel dilation, and impaired vessel integrity, or if these phenotypes might be secondary to other failed TGFβ-dependent functions (Folkman and D'Amore, 1996; Li *et al.*, 1999; Oh *et al.*, 2000).

TGFβ superfamily signaling is attenuated through a distinct cohort of negative Smad proteins, one of which is Smad7 (Afrakhte *et al.*, 1998; Christian and Nakayama, 1999; Hayashi *et al.*, 1997; Itoh *et al.*, 1998; Massague, 1998; Massague and Chen, 2000; Nakao *et al.*, 1997; Nakayama *et al.*, 1998a; Nakayama *et al.*, 1998b; Topper *et al.*, 1997; Tsuneizumi *et al.*, 1997). Smad7 blocks signaling by ligands of the TGFβ, activin and BMP families. Since Smad7 expression is upregulated in response to these signals, it likely acts as a negative feedback regulator of this system (Afrakhte *et al.*, 1998; Bhushan *et al.*, 1998; Casellas and Brivanlou, 1998; Ebisawa *et al.*, 2001; Ishisaki *et al.*, 1998; Ishisaki *et al.*, 1999; Itoh *et al.*, 1998; Kavsak *et al.*, 2000; Massague, 1998; Massague and Chen, 2000; Miyazono, 2000; Nakao *et al.*, 1997; Nakayama *et al.*, 2001). In the vasculature, Smad7 is normally expressed in endothelial cells of developing and mature vessels, and can be induced by vascular flow shear stress as well as TGFβ signals (Topper *et al.*, 1997; Zwijsen *et al.*, 2000). During development Smad7 is more highly expressed in endothelial cells of larger blood vessels, perhaps because of their exposure to greater blood flow (Zwijsen *et al.*, 2000).

Since Smad7 broadly inhibits TGFβ superfamily signaling, we hypothesized that misexpressing Smad7 would allow us to generate additional insights into vascular development than are provided by manipulation of more pathway-specific TGFβ superfamily signaling components. Here we show that misexpression of Smad7 during angio-

TABLE 1
Effects of RCAS Virus-Mediated Gene Misexpression on Limb Vessels

Virus	Time postinfection (hours)	N	Wide SCA only	Wide PMV only	Wide SCA + PMV only	AVS (with wide SCA + PMV)	Distal VS and wide PMV	No effect
Smad7	24	20	4	10	2	—	—	4
	48	28	8	2	4	10	2	2
	72	27	1	5	3	9	9	—
Noggin	24	14	—	—	—	—	—	14
	48	7	—	—	—	—	—	7
	72	6	—	—	—	—	—	6
BMPR Ib^{DN}	24	3	—	—	—	—	—	3
	48	3	—	—	—	—	—	3
	72	4	—	—	—	—	—	4
GFP	24	3	—	—	—	—	—	3
	48	6	—	—	—	—	—	6
	72	6	—	—	—	—	—	6

Note. Numbers and types of vascular defects obtained following RCAS virus infection between HH s17–20, harvested at indicated times. N–number; SCA–subclavian artery; PMV–posterior marginal vein; AVS–arterio-venous shunt; VS–intervenous shunt.

genic remodeling of the embryonic chick vasculature induces dilated vessels, as well as severe vascular malformations including arteriovenous shunts reminiscent of AVMs. These phenotypes can be prevented by concomitant activation of the intracellular BMP signaling pathway. Smad7-infected vessels are not hemorrhagic, enlarge independently of VSMCs and do not have defects in VSMC recruitment. Thus, our results suggest that the principle role of TGFβ superfamily signals during early embryonic angiogenesis and vascular remodeling is to regulate vessel caliber and connectivity through the Smad1/Smad5/Smad8 intracellular pathway. They also suggest that VSMCs do not control vascular size or integrity in early development.

MATERIALS AND METHODS

Embryology

Fertile White Leghorn chick eggs (SPAFAS) were incubated at 38°C in a humidified, forced air incubator. Experimental manipulations were performed from HH st15 to HH st21 and embryos were harvested through 72 h postmanipulation (Hamburger and Hamilton, 1951).

The vasculature was visualized either by India ink (1:2 v/v dilution in Ringer's saline) or fluorescein-conjugated Ricinus lectin (Vector labs; 1:5 v/v dilution in Ringer's saline) injection into the vitelline vein (Thurston *et al.*, 1996). India ink injected embryos were fixed immediately in 5% (w/v) trichloroacetic acid, dehydrated in ethanol and cleared in methyl salicylate. Lectin injected embryos were fixed in Dents fix (20% DMSO in methanol) after 10 min incubation at room temperature, dehydrated, and cleared in benzyl alcohol:benzyl benzoate (1:2 v/v; BABB).

Virology

An RCAS BP(B)Smad7 virus (Smad7 virus) was constructed by subcloning the open reading frame of the *Xenopus* Smad7 gene (initially called xSmad8) into the RCAS BP(B) retroviral vector via a pSlax13 shuttle vector intermediate (Logan and Tabin, 1998; Nakayama *et al.*, 1998b; Souchelnytskyi *et al.*, 1998). The RCAS BP(A)noggin, RCAS BP(A)BMPR Ia^{CA}, RCAS BP(A)BMPR Ib^{DN}, RCAS BP(A)BMPR Ib^{CA}, RCAS BP(A)GFP and RCAS BP(B)GFP viruses were described previously (Capdevila and Johnson, 1998; Logan *et al.*, 1998; Zou *et al.*, 1997). Concentrated virus stocks were generated using standard procedures, and all stocks used had titers of at least 5×10^8 infectious units/ml (Logan and Tabin, 1998).

To target the head, the brain ventricles of HH st15 embryos were filled with viral supernatant. For single virus limb infections, virus was injected into HH st17 through st21 wing buds. Injections were targeted such that either the entire limb or specific subregions were infected with virus. For double virus limb infections, equal volumes of an A coat virus and the Smad7 B coat virus were mixed and injected using the same procedure as for single virus injections. In each experiment positive control Smad7 infections were performed in parallel. When phenotypic suppression was observed, efficient infection of both viruses was confirmed using a subset of the injected embryos. Targeting was monitored by nonradioactive whole mount *in situ* hybridization using either a pan-retroviral or an insert-specific *in situ* probe (Riddle *et al.*, 1993). Virus distribution in tissue sections was determined by immunostaining with the anti p19^{gag} monoclonal antibody 3C2 (Potts *et al.*, 1987).

Immunohistochemistry

Tissue for section immunocytochemistry was fixed in 4% paraformaldehyde in PBS and either dehydrated through 30% sucrose

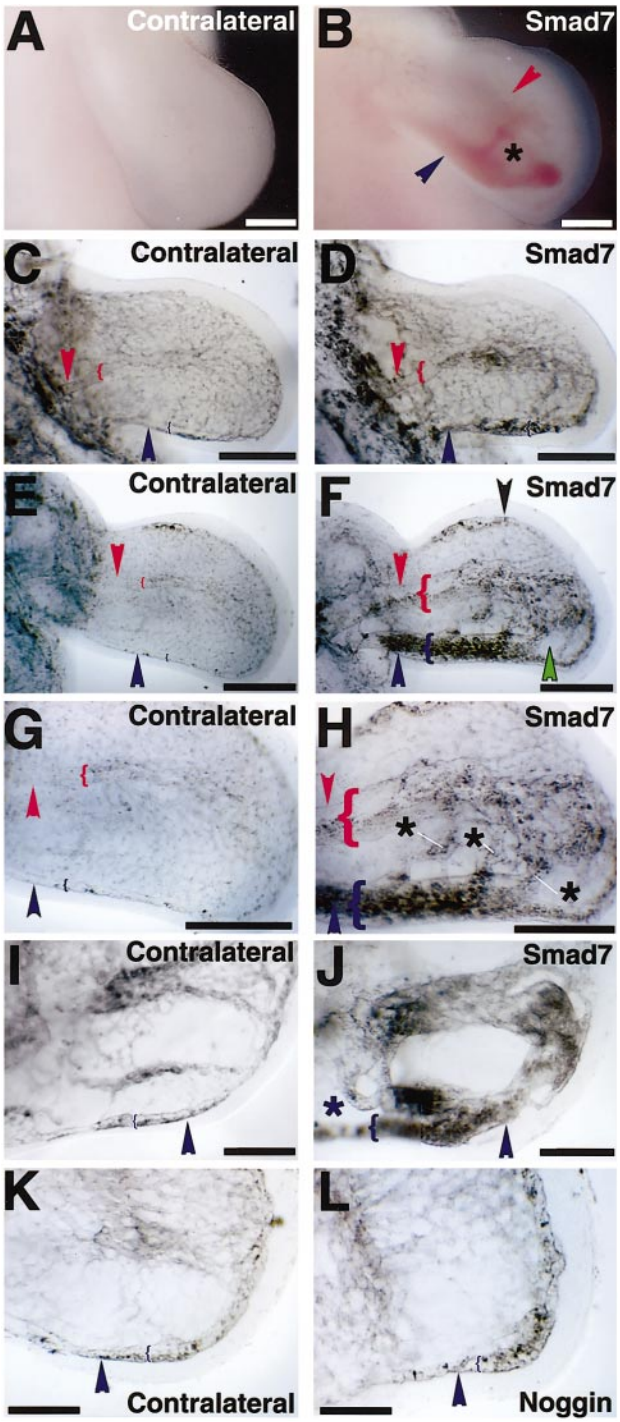

FIG. 1. Ectopic Smad7 expression induces vascular defects in the limb. Right forelimb infected throughout limb mesenchyme at HH st17, 24–72 h postinfection. A-B: Live view of control (A) and Smad7 virus-infected (B) limbs 48 h postinfection, showing large volume of blood in enlarged subclavian artery (SCA; red arrowhead) and posterior marginal vein (PMV; blue arrowhead) that have merged (black asterisk). C-L: India ink-stained limb vasculature. C, E, G, I, K: Control limbs; D, F, H, J: Smad7 virus-infected limbs; L: Noggin virus-infected limb. At 24 h postinfection, (D) SCA and PMV are enlarged relative to control vessels (C), but lack obvious intervascular shunts (SCA and PMV width demarcated by red or blue brackets respectively). At 48 h postinfection (F) massively enlarged subclavian artery and posterior marginal vein are connected via a shunt in the central region of the limb, and are significantly closer than in control limb (E). In proximal, anterior and distal mesenchyme enlarged but tortuous looking vessels are evident (F; black arrowhead). Abnormal avascular spaces are also visible between distal blood vessels (F; green arrowhead). (H) A higher magnification view of (F) shows the enlarged SCA, enlarged PMV and multiple intervascular shunts between the SCA and PMV (black asterisks). (J) Smad7 virus infected hand plate at HH st24 exhibiting massively enlarged PMV and vascular shunts between the posterior marginal and interdigital veins. Also note shunting between the PMV and interdigital vein (blue asterisk). (K) Noggin virus-infected limb at HH st18 fixed after 72 h has truncated, widened limb, with normal vasculature and no enlarged blood vessels or visible shunts. Scale bars: 500 μm.

for cryosectioning or graded alcohols for paraffin embedding. Cryosections were cut at 12 μm and paraffin sections at 8 μm for use in immunocytochemistry using standard procedures. For virus detection 3C2 hybridoma supernatant was used at 1:15 dilution. Murine monoclonal anti-smooth muscle alpha actin, clone 1A4 (Sigma) was used at 1:850. Cy3-conjugated goat anti-mouse IgG secondary antibody (Jackson ImmunoResearch, West Grove, PA, USA) was used at 1:1000.

Embryos were processed for whole mount antibody staining as described by Kardon (1998). Briefly, embryos were fixed overnight in Dents fix then placed in Dents bleach (1:2 v/v; 30% H_2O_2: Dents Fix) overnight. Embryos were rinsed in PBS, blocked in 5% sheep serum: 20% DMSO in PBS then stained overnight with anti-smooth muscle alpha actin antibody (1A4; 1:1000). Embryos were washed in PBS, stained overnight with Cy3 goat anti-mouse IgG (1:1000), washed in PBS, dehydrated, cleared in BABB and photographed using a Nikon Eclipse 800 fluorescence photomicroscope or a Biorad MRC 500 confocal microscope.

Transmission Electron Microscopy

At various times following Smad7 virus infection, limbs were fixed at 4°C for 2.5 h in a solution of 2.5% paraformaldehyde: 2% gluteraldehyde in 0.1M phosphate buffer (PB) (Fallon and Kelley, 1977). Following rinsing in PB, they were processed and epoxy resin embedded for electron microscopy as described (Fallon and Kelley, 1977). 10μm sections were cut with a glass knife until the correct location was attained and then 80 nm sections collected and viewed with a JEOL 1200EX transmission electron microscope. Endothelial cells lining the subclavian artery of Smad7 virus-infected and control limbs were identified by location and morphology. Endothelial cell counts were performed on directly visualized TEM images, while interendothelial junctions were assessed and counted on composite TEM micrographs.

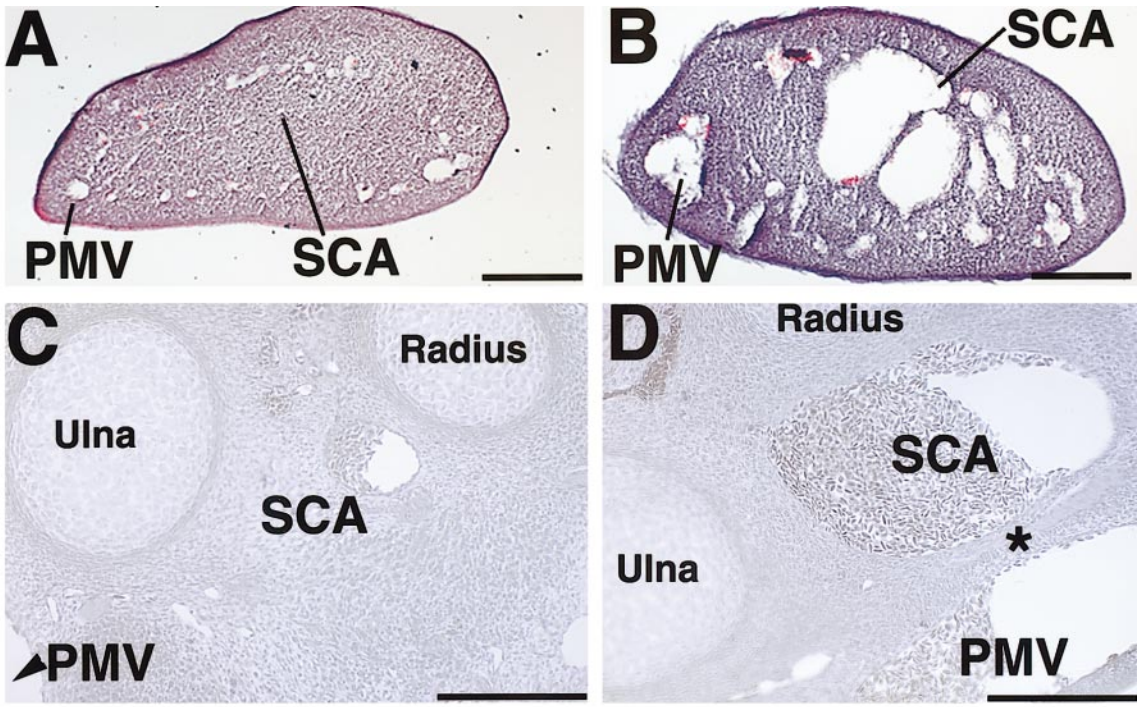

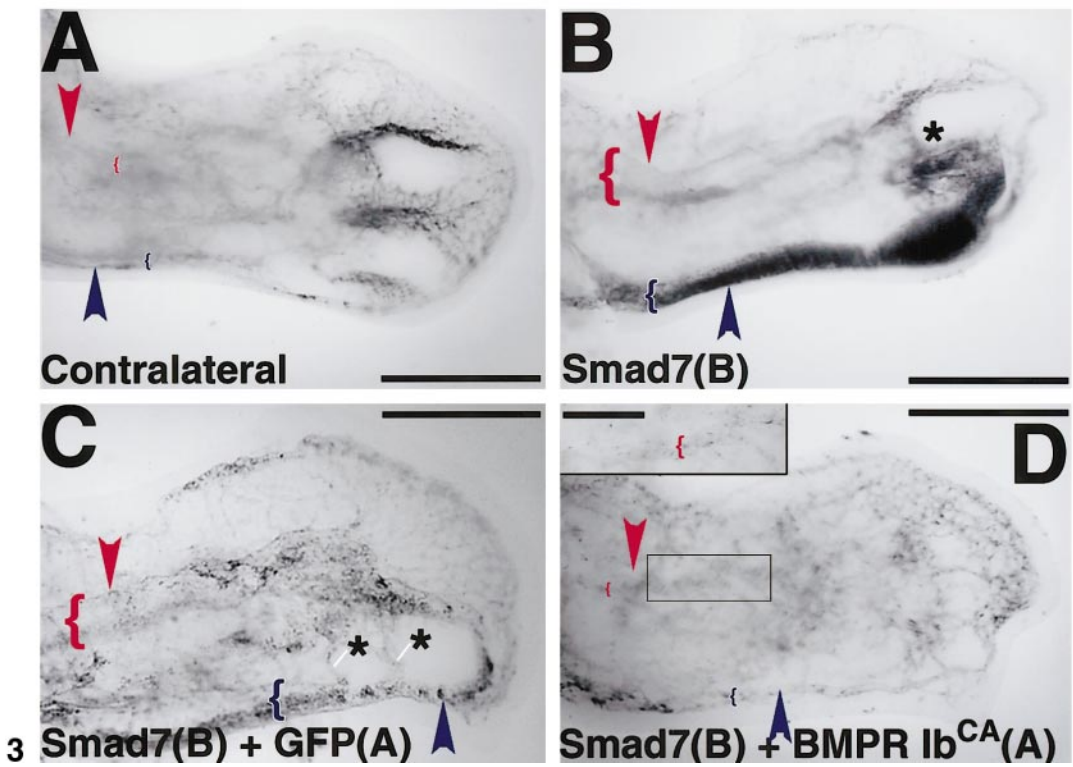

FIG. 2. Smad7 virus infection causes substantial dilation of subclavian artery and posterior marginal vein. Transverse sections through distal (A-B) or proximal region (C-D) of control or HH st17 Smad7 virus-infected limb. A-B: Eight micrometers hematoxylin counterstained sections, 48 h postinfection. Subclavian artery (SCA) and posterior marginal vein (PMV) are enlarged and closer in Smad7 virus-infected (B) limb than control limb (A). The control SCA is very small due to distal location of the limb section, and was traced through adjacent proximal sections, while in the infected limb almost all of the blood vessels are enlarged. In addition the SCA appears to be merging with many adjacent vessels. C-D: Ten micrometers osmium tetroxide counterstained sections, 72 h postinfection. In the control limb (C) the SCA is located between the radial and ulnar cartilage anlagen. The SCA and PMV are displaced towards one another in the Smad7 virus-infected limb (D), and are enormously enlarged and might be fusing into an arterio-venous malformation (asterisk). Scale bars: 200 μm.

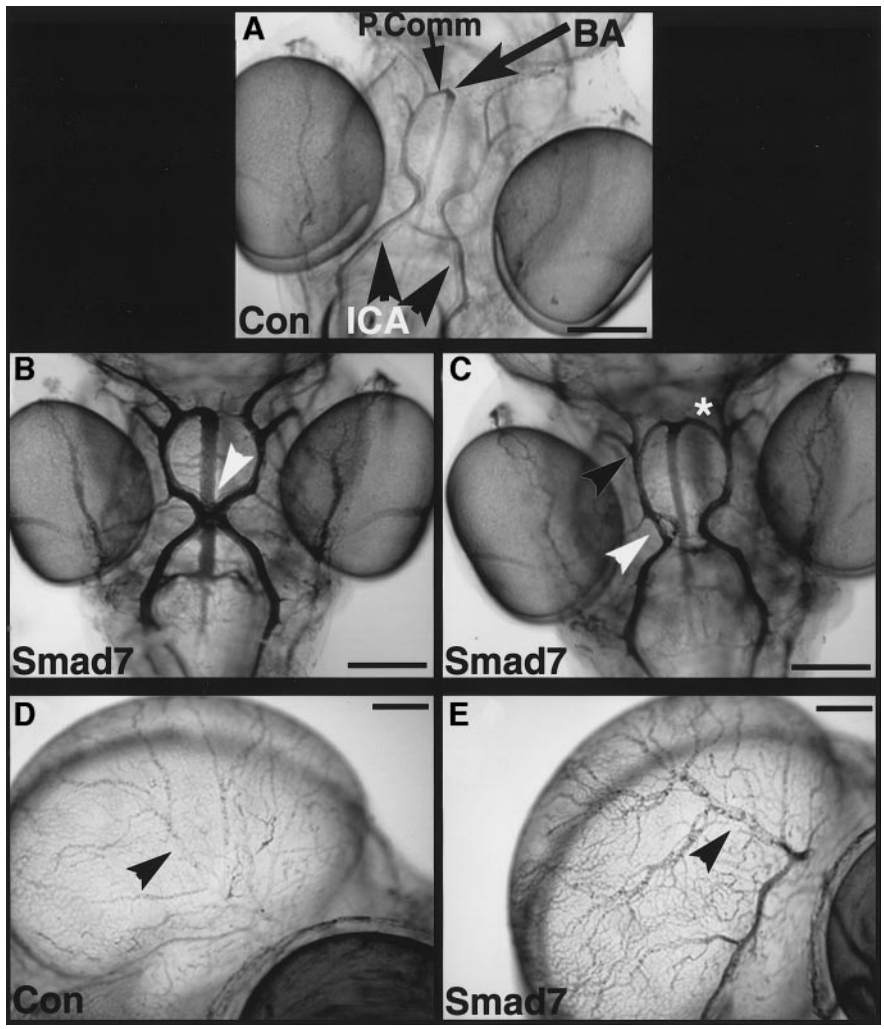

FIG. 4. Smad7 induces dilated and merged arteries in the developing head. A-E India ink-labeled blood vessels of embryos infected in brain ventricles with Smad7 virus. A-C: Dorsal view through the hindbrain A) Uninfected control head. The major arteries–the right and left internal carotid arteries (ICA; arrowheads) are separate and the basilar artery (BA; arrow) is small and has asymmetric posterior communicating arterial connections (P. Comm; arrow) to the ICAs. B-C: Ventricular infection at HH st15, 72 h postinfection. (B) The BA and ICAs are significantly enlarged, and the ICAs have merged (white arrowhead). (C) The BA and ICAs are enlarged and the ICAs are not fused. However, the left ICA has an intra-arterial shunt (white arrowhead) and the branching pattern of the left ICA at the cranial ramus of the Circle of Willis is abnormal (black arrowhead). Furthermore, the right posterior communicating artery (white asterisk) is abnormally dilated. D-E: Lateral views of vasculature supplying midbrain, ventricular infection at HH st18, 48 h postinfection. Smad7 virus-infected head (E) has enlarged vessels and changed vascular branching patterns relative to the control head (D) (black arrowhead). Scale bars: 500 μm.

FIG. 3. Vascular defects induced by Smad7 are prevented by co-injection of constitutively active BMPR Ib. A-D: India ink-labeled blood vessels of limbs fixed 72 h after virus injection at HH st20. A: Uninfected limb, contralateral to limb in panel B. Position and width of SCA (red arrowhead and red bracket) and PMV (blue arrowhead and blue bracket) as indicated; B: Smad7(B) virus-infected limb. Note widened SCA and PMV and vascular shunt (black asterisk); C: Limb following coinjection of Smad7(B) virus and GFP(A) virus. Note the widened PMV, SCA and vascular shunt, and the similarity in phenotype severity to Smad7 virus-infection; D: Limb following injection of Smad7(B) and BMPR Ib^{CA}(A). Note no widened vessels, no connectivity defects and apparently normal vascular architecture, however, the distal part of the limb is truncated. The inset box shows higher magnification image of proximal limb indicating SCA is not enlarged. SCA–subclavian artery; PMV–posterior marginal vein. Scale bars: 500 μm A-D, 250 μm inset.

TABLE 2
Coexpression of Constitutively Active BMP Receptors Prevents the *Smad7*-Induced Vascular Defects

Virus	Time postinfection (hours)	N	Wide SCA only	Wide PMV only	Wide SCA + PMV only	AVS (with wide SCA + PMV)	Distal VS and wide PMV	Limb truncation	No effect
Smad7(B)	24	6	1	3	—	—	—	—	2
	48	6	1	1	—	2	—	—	2
	72	7	—	3	—	2	1	1	—
Smad7(B) + *BMPR Ia*^{CA}(A)[a]	24	5	—	—	—	—	—	1	4
	48	5	—	2	1	1	—	1	—
	72	7	—	2	1	2	—	2	—
Smad7(B) + *BMPR Ib*^{CA}(A)	24	4	—	—	—	—	—	2	2
	48	5	—	—	—	—	—	5	—
	72	8	—	3	—	—	—	5	—
Smad7(B + *BMPR Ib*^{DN}(A)	24	3	—	—	1	—	—	—	2
	48	3	1	—	—	1	—	1	—
	72	5	—	1	—	4	—	—	—
Smad7(B) + *GFP*(A)	24	4	1	1	—	—	—	—	2
	48	4	—	2	—	1	—	—	1
	72	6	1	1	—	2	1	1	—

Note. Numbers and types of vascular defects obtained following RCAS (B) or simultaneous RCAS (A) and (B) subtype double virus combinations as indicated. Embryos were infected between HH s18–21 and harvested post-infection at indicated times. The *Smad7*(B) data presented here are also incorporated into Table 1. Abbreviations as in Table 1.

[a] Vascular phenotypes observed with this virus combination were of a milder nature compared to *Smad7* virus alone.

Morphometric Analysis

Digital images of 8 μm transverse sections were collected, and blood vessel dimensions measured using NIH Image 1.61 software. For each Smad7 virus-infected limb a proximal section that contained the largest vessels near the entry point of the subclavian artery into the limb was chosen, and area and perimeter of the subclavian artery and posterior marginal vein were measured. Vessels in an equivalently positioned section from the contralateral control limb were also measured. A minimum of six Smad7 virus-infected and control limbs were analysed at each time point examined.

RESULTS

Ectopic Smad7 Expression Causes Defects in Limb Vasculature

A replication-competent RCAS avian retrovirus that expresses the *Xenopus* Smad7 gene was constructed to investigate the consequences of blocking TGFβ superfamily signaling during avian development. The *Xenopus* gene was

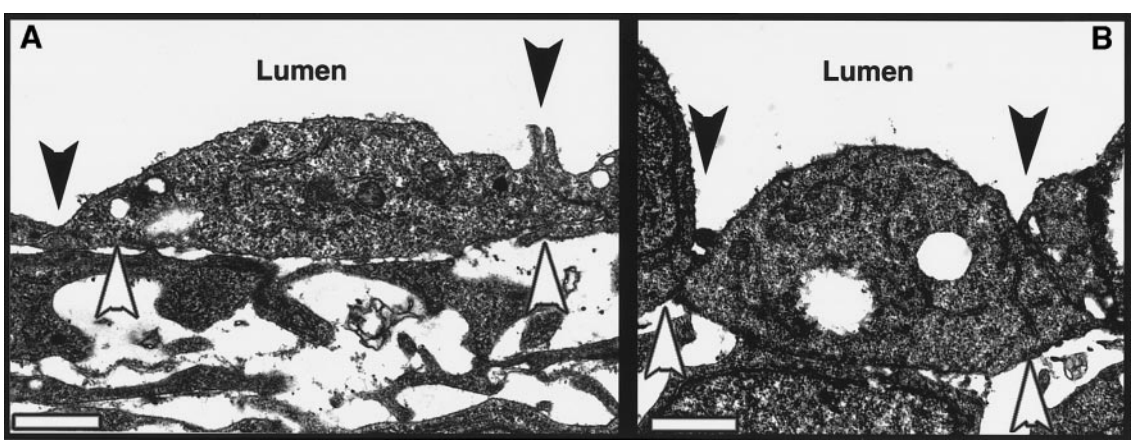

FIG. 5. Transmission electron micrographs showing intact vessels and presence of intercellular junctions. A-B: TEM micrograph of subclavian artery, HH st17 limb infection, 72 h postinfection. Endothelial cells lining the subclavian artery of control (A) and Smad7 virus-infected (B) limbs. In both control and Smad7 virus-infected vessels, endothelial cells are tightly associated and have intact junctions between endothelial cells (black arrowheads). Moreover the endothelial cells are present as a monolayer and have an apparently continuous and intact basement membrane (white arrowhead). Red blood cells are observed only in the vessel lumen. Scale bar: 1 μm.

used because its activity is well characterized, and so that exogenous transcripts could be distinguished from those of the endogenous Smad7 gene (Nakayama *et al.*, 1998b). Limb primordia were injected with Smad7 virus at HH st17 to st21 after the onset of angiogenesis, and examined from 24 to 72 h later. Immunostaining for expression of a viral-specific epitope or whole mount *in situ* analysis using a viral-specific probe revealed that both vascular endothelium and surrounding nonvascular tissue are infected with Smad7 virus (data not shown).

Infection by this protocol causes striking vascular defects. As early as 24 h postinfection, an apparent pooling of blood in central and proximal posterior limb regions was consistently observed in living embryos. By 48 h postinfection the major vessels, particularly the subclavian artery and posterior marginal vein, were visibly enlarged and displaced towards the dorsal limb surface ($n > 600$; Fig. 1A, B). Despite these gross vascular defects, no edema or inflammation of surrounding tissue was observed.

To visualize the entire vasculature, India ink was injected into the vitelline vein and the embryos cleared. Limbs were scored for alterations in vessel size and connectivity (Table 1). Major vessel enlargement is visible within 24 h postinfection (Fig. 1C, D), and by 48 h the subclavian artery and posterior marginal vein are dilated into huge tube-like structures, and can be displaced towards one another (Figs. 1E, F). Examination of vessels in sectioned limb tissue confirms that vessel caliber is substantially increased (Fig. 2). The subclavian artery and posterior marginal vein can be either independently or simultaneously affected. In addition, smaller vessel organization in proximal and distal regions of the limb is disrupted, and some of these vessels are enlarged and appear tortuous (Fig. 1F). There are also abnormally wide avascular spaces separating the vessels, suggestive of reduced angiogenic remodeling (Fig. 1F). The independence of the vascular dilation phenotypes was confirmed by targeting virus in some embryos to either the central or posterior limb tissue. In these instances only the major vessel in the targeted area is dilated (not shown).

Vascular shunts that bypass the capillary beds between the arterial and venous circulations are also often observed. They are particularly evident from 48 h postinfection between the subclavian artery and posterior marginal vein in central or distal regions of the limb (Figs. 1F, H and 2C, D). Intervenous shunts also form distally between the posterior marginal vein and interdigital veins. These venous shunts can form either in addition to or independently of arteriovenous shunts (Fig. 1H, J). While vessel enlargement can occur in the absence of obvious vascular shunting, we do not observe shunting in the absence of enlarged vessels. Furthermore there is a general progression of vascular abnormalities from dilation to simple and then complex shunting with time (Fig. 1, Table 1).

The Effects of Smad7 Misexpression Are Not Phenocopied by BMP Signaling Antagonists

To assess whether these vascular defects are specific to Smad7 misexpression, we infected limb tissue with several other RCAS viruses. Infection with an RCAS-GFP virus did not cause any reproducible vascular malformations, indicating that RCAS virus infection alone does not perturb vascular development. To test whether antagonism of BMP signaling can cause similar vascular defects, we misexpressed the BMP binding protein noggin or a dominant negative form of BMPR Ib (BMPR Ib^{DN}) using a similar retroviral infection strategy. Neither virus caused significant vascular defects (Fig. 1K and Table 1).

While they did not all cause vascular defects, the noggin, BMPR Ib^{DN} and Smad7 viruses did induce similar defects in other aspects of limb development. The noggin virus-infected limbs are truncated, have a thickened AER, decreased expression of Shh pathway components, reduced programmed cell death and do not develop cartilage condensations. The BMPR Ib^{DN} virus caused similarly truncated and broadened limbs (data not shown). These observations are consistent with previous reports using these viruses (Zou *et al.*, 1997; Capdevila and Johnson, 1998; Pizette and Niswander, 1999). Smad7 virus-infected limbs exhibit phenotypes very similar to those caused by noggin misexpression, and will be described in detail elsewhere (data not shown; manuscript in preparation). Taken together these data suggest that while Smad7 can effectively block BMP signaling in the limb, the additional vascular defects are not due to blocking BMP signals.

Intracellular BMP Pathway Activation Prevents Smad7-Induced Vascular Defects

Our data suggest that antagonizing TGFβ superfamily signaling causes severe vascular defects. If this is the case, then simultaneous intracellular activation of a positive Smad signaling pathway might prevent or reduce the Smad7-induced vascular phenotypes. To test this hypothesis we used a viral coinfection strategy. The RCAS Smad7 virus has a B subtype envelope, and thus A subtype viruses can superinfect Smad7(B) virus-infected cells. We combined Smad7(B) virus with various RCAS(A) subtype viruses encoding constitutively active (CA) or dominant negative BMP receptors and infected limb buds with the multivirus cocktails.

Coinfection of Smad7(B) and BMPR Ib^{CA}(A) viruses resulted in essentially normal vessel morphology, even 72 h after infection. Neither the subclavian artery nor the posterior marginal vein is significantly enlarged, and intervascular shunting is absent (Fig. 3; Table 2). Some distal truncation of the limb mesenchyme is observed. This is similar to the effects caused by weak infection with the BMPR Ib^{CA}(A) virus alone (Zou *et al.*, 1997). A similar result was observed when BMPR Ia^{CA}(A) was introduced in com-

bination with Smad7(B) (Table 2). However, in this case mild vessel dilation and shunt formation is occasionally observed. Infection with either of the constitutively active BMPR viruses alone leads to severe defects in limb outgrowth and tissue differentiation (data not shown; Zou *et al.*, 1997). Thus, their effects on vascular development could not be easily assessed. Smad7(B) virus in combination with either BMPR Ib^{DN}(A) or GFP(A) virus resulted in vascular defects similar in frequency and severity to infection with Smad7(B) virus alone (Table 2). Suppression of the Smad7 virus induced phenotype is thus specific to simultaneous activation of the intracellular BMP signaling pathway, and is not attributable to dilution or competition by the (A) coat viruses.

Smad7 Infection Causes Vascular Malformations in the Developing Brain

To ascertain if Smad7 misexpression could cause similar vascular abnormalities in other regions of the embryo, the developing brain ventricles were injected with Smad7 virus at HH st15. Only angiogenesis and angiogenic remodeling events are occurring at this stage of cranial vessel development (Hughes, 1934; Pardanaud *et al.*, 1987; Coffin and Poole, 1988; Pardanaud *et al.*, 1989; Poole and Coffin, 1989; Risau, 1997). As in the limb, vascular defects are observed as early as 24 h postinfection (Fig. 4). In the majority of cases the basilar and internal carotid arteries are dilated (Table 3). The right and left internal carotid arteries are also frequently displaced medially towards each other, and by 48 h postinfection can merge abnormally, forming arterial anastomoses and premature connections between the left and right cranial circulations (Fig. 4A-D; Table 3). In addition intra-arterial shunts fusing back to the same vessel are observed (Fig. 4D; Table 3). The major vascular branches supplying blood to the midbrain are also enlarged, with reduced branch formation and apparent intravascular shunting ($n = 4/4$; Fig. 4E,F).

Thus, Smad7 misexpression causes vascular dilation, fusion, and shunt formation in multiple regions of the embryo. Moreover, appropriate physical separation between the major vessels is not maintained, since the relative positions of the right and left internal carotid arteries in the head and the subclavian artery and posterior marginal vein in the limb are frequently perturbed (Figs. 1F; 4B,C).

Smad7 Virus-Infected Blood Vessels Are Intact and Are Not Hemorrhagic

In mice mutant for TGFβ ligands or receptors, as well as in human HHT patients, blood vessels lack structural integrity and hemorrhage blood into the surrounding mesenchyme (Dickson *et al.*, 1995; Oshima *et al.*, 1996; Shovlin and Letarte, 1999). Therefore, we asked whether Smad7 misexpression causes similar gross defects in vessel integrity. India ink or fluorescently labelled Ricinus lectin was injected into the embryonic circulation of Smad7 virus-infected embryos (Thurston *et al.*, 1996). Neither stain penetrated beyond the vascular lumen when examined in whole mount or sectioned limb tissue (Fig. 1 and data not shown). In addition no signs of hemorrhage were observed in sectioned tissue (Fig. 2).

We also examined vessel integrity by transmission electron microscopy (TEM). In electron micrographs blood cells are observed only inside the vessels, consistent with the ink and lectin injection results (Fig. 5). Furthermore interendothelial cell junctions, which prevent the passage of blood cells outside the endothelium and help maintain the integrity of the endothelial layer, are visible between all endothelial cells lining the dilated infected vessels (166 endothelial cell junctions examining in infected tissue vs. 56 in control tissue; Fig. 5A, B). In addition the basement membrane underlying the endothelial cells appears intact (Fig. 5A, B). Thus, from analysis of several independent criteria, vessel integrity is not grossly compromised by Smad7 misexpression, despite severe defects in vessel size and connectivity.

Endothelial Cell Morphology Lining Smad7 Virus-Infected Vessels Appears Normal

To determine if increased vessel size correlates with changes in endothelial layer morphology, we examined Smad7 virus-infected vessels by TEM and light microscopy. In addition to the presence of endothelial cell junctions and a normal basement membrane, the endothelial cells have typical endothelial morphology, with a centrally located nucleus, are of normal size and are present in a monolayer (Fig. 5).

Blood vessel size was measured in limbs harvested at various times following Smad7 virus infection. Limbs were sectioned transversely across the major vessel axis, and perimeters and cross-sectional areas of the subclavian artery and posterior marginal vein determined (Fig. 6A, B). Both perimeter and area of infected vessels are larger than control limbs from 18 h postinfection, and continue to increase through 72 h postinfection, the latest time point examined (Fig. 6A, B). At this time mean perimeter is increased approximately 2.8-fold and mean vessel area is increased approximately sevenfold relative to control vessels.

The apparently normal endothelial cell morphology combined with the enlarged vessel size suggested that affected vessels contain more endothelial cells. Therefore, we counted endothelial cells in TEM micrographs of subclavian arteries of Smad7 virus-infected and control limbs. Smad7 virus-infected vessels contain approximately 2.5-fold more endothelial cells than control vessels at 72 h postinfection (87 ± 4.3 cells per section[mean $\pm$ SEM] in infected tissue, $n = 9$; vs. 34 ± 1.3 cells in control tissue, $n = 8$). Electron micrographs were used as we lack a reliable immunochemical marker of chick endothelial cells that

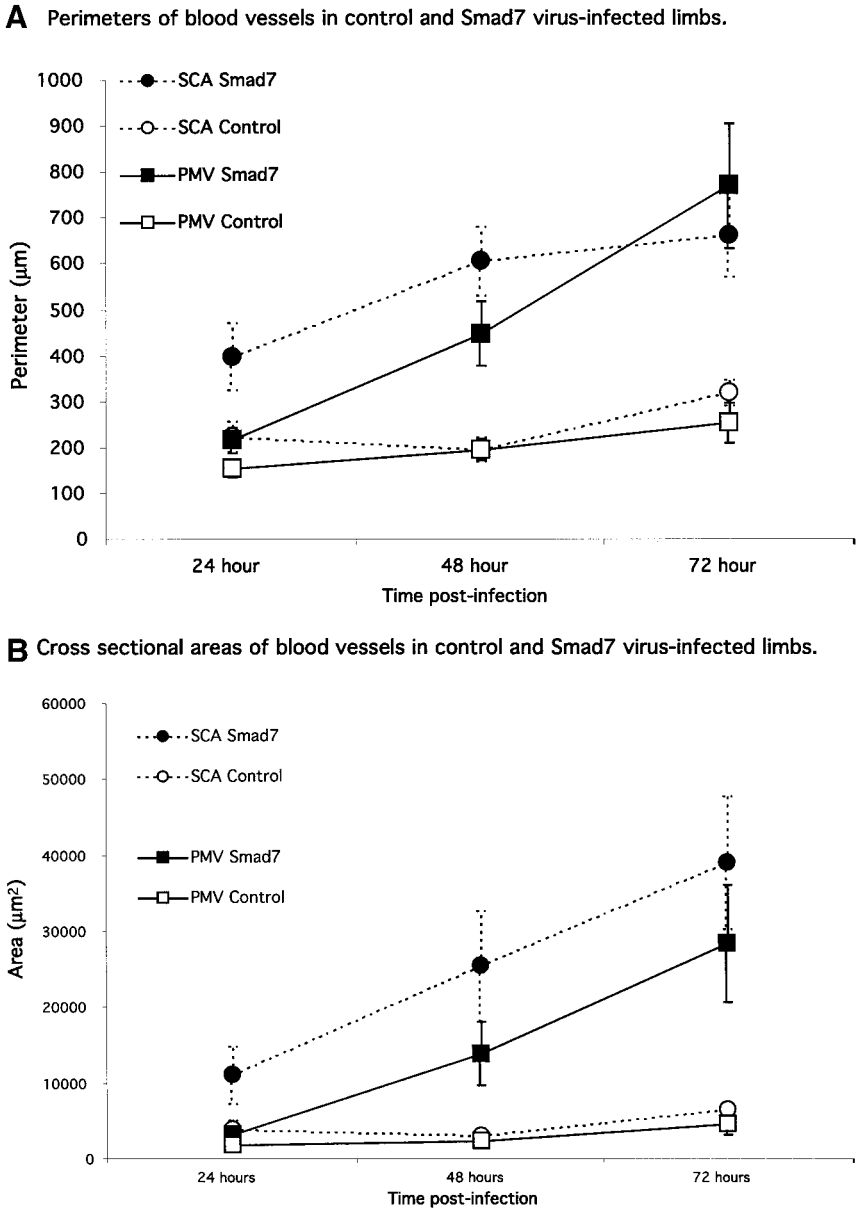

FIG. 6. Changes in vessel size following Smad7 virus infection. Perimeters (A) and cross-sectional areas (B) of subclavian arteries and posterior marginal veins of Smad7 virus-infected and control limbs from 24 to 72 h after virus infection. SCA–subclavian artery; PMV–posterior marginal vein. Values shown are mean ± SEM. N ≥ 6 for each value.

also allows unambiguous cell counts. However, in preliminary studies we have also counted endothelial cells identified in paraffin embedded tissue sections based on cell morphology, and find an increase in cell number consistent with the increases in perimeter from 24 through 72 h postinfection (data not shown). As the mean changes in perimeter length and endothelial cell number are similar, the endothelial cell density in Smad7 virus-infected limbs is essentially unaffected. Taken together the cell density, vessel morphology and vascular integrity data suggest that Smad7 misexpression causes gross dilation of otherwise normal endothelial tubes.

Vessel Widening Is Independent of Vascular Smooth Muscle

In mouse mutants as well as human diseases with defects in TGFβ superfamily signaling that display an enlarged and

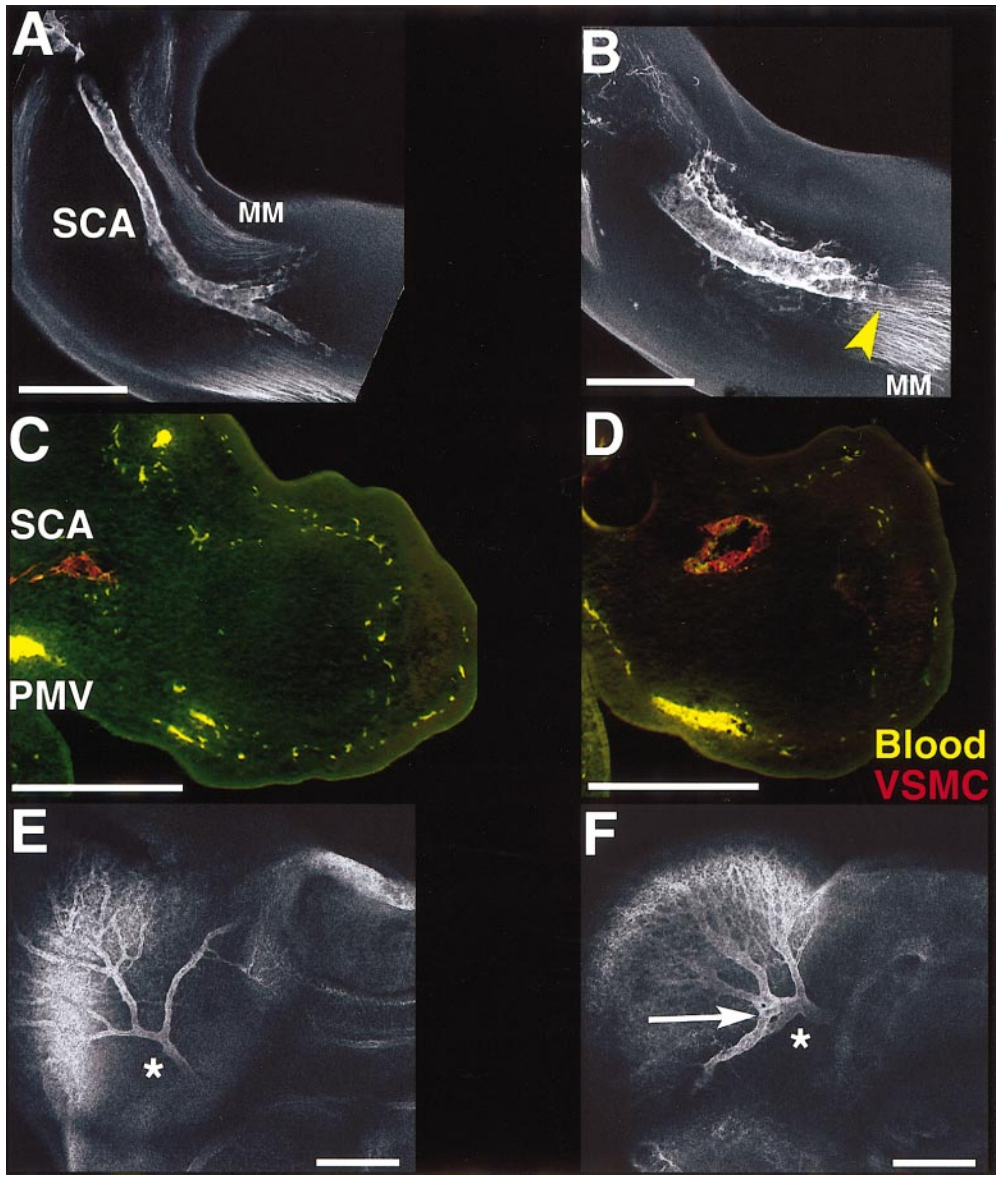

FIG. 7. Smad7 misexpression does not affect vascular smooth muscle. Immunofluorescent staining of smooth muscle alpha actin (SMA) expression following Smad7 virus-infection of embryonic chick limbs and heads. A-B: Confocal images of control (A) and Smad7 virus-infected (B) whole mount limbs infected at HH st17, 72 h postinfection. SMA expression is detected surrounding both normal (A) and dilated (B) subclavian arteries (SCA) and just beyond the branchpoint of the ulnar and radial arteries. The distal extent of SMA immunoreactivity is shown. Staining also extends proximally to the base of the limb, but is out of the focal plane of the image. Some immunoreactivity is also seen in the dorsal and ventral muscle masses (MM). Proximal is to left in both images. C-D: Transverse sections of limb tissue at entry point of SCA in limb. Control (C) and Smad7 virus-infected (D) limb sections, infected at HH st17, 48 h postinfection. Both control and enlarged, infected SCAs are surrounded by a similar extent of SMA immunoreactivity, and no other vessels stain positive for SMA. The posterior marginal vein (PMV) in (D) is also enlarged. Neither affected nor control PMVs show any SMA staining. E-F: Confocal images of whole mount control (E) and Smad7 virus-infected (F) heads, infected at HH st18, 48 h postinfection. SMA staining covers the vascular branch supplying blood to the developing midbrain (asterisk), as well as the capillaries covering the midbrain in both images. In the virus-infected head the vascular branch is widened (asterisk), has a less complex branching pattern, and has an intravascular shunt (arrow). Scale bars: 200 μm.

TABLE 3
Effects of RCAS-Smad7 Virus Infection on Hindbrain Vessels

Time (hours)	Phenotype			
	ICA dilated	ICA merged	ICA shunts	BA dilated
24	1/3	0/3	0/3	0/3
48	10/11	6/11	0/11	10/11
72	9/11	8/11	2/11	9/11
Total	20/25 80%	14/25 56%	2/2 58%	19/25 76%

Note. Number and frequency (%) of enlarged vessels and vascular malformations observed following *Smad7* virus-infection of brain ventricles harvested at various times after HH s15–17 infection. ICA–Internal carotid artery; BA–Basilar artery.

hemorrhagic vessel phenotype there is a loss or disorganisation of vascular smooth muscle cells associated with the affected vessels (Chang *et al.*, 1999; Dickson *et al.*, 1995; Li *et al.*, 1999; Oh *et al.*, 2000; Shovlin and Letarte, 1999; Urness *et al.*, 2000; Yang *et al.*, 1999). Thus, TGFβ superfamily signaling might be required for VSMC recruitment and maintenance, and VSMC-endothelium interactions might be required to maintain vascular integrity (Folkman and D'Amore, 1996).

To determine whether the vascular phenotypes correlate with changes in recruitment or loss of VSMC, the expression of smooth muscle alpha actin, a marker of differentiated VSMC, was examined by whole mount and section immunohistochemistry in Smad7 virus-infected and control limbs from HH st20 through HH st30 (Fig. 7). In control HH st20 limbs, smooth muscle alpha actin expression is detected only in tissue surrounding the proximal region of the subclavian artery, and is absent from the remaining limb vasculature. As limb development proceeds, this expression is detected progressively more distally surrounding the subclavian artery, and its major branches, the radial and ulnar arteries (Fig. 7A). At the latest developmental stages examined, some expression is also observed in association with secondary arterial branches. However, the majority of vessels in the limb, including the posterior marginal vein, are devoid of differentiated VSMCs from HH st20 through HH st30 (Fig. 7A, C). Thus, unlike in many other regions of the embryo, there is a prolonged time period between the formation of the limb vasculature and its association with differentiated smooth muscle cells. Since Smad7 virus infection causes posterior marginal vein dilation without gross loss of integrity prior to HH st30, differentiated VSMCs must not be required to maintain either the caliber or integrity of these vessels. However, VSMC precursors that do not yet express smooth muscle alpha actin might be associated with these vessels.

Examination of smooth muscle alpha actin immunoreactivity in Smad7 virus-infected limbs reveals little, if any, alteration compared to control limb staining patterns, despite the dramatic effects of Smad7 misexpression on vessel caliber. In Smad7 virus-infected limbs the enlarged subclavian artery is surrounded by VSMCs, and the spatial distribution and proximo-distal temporal progression of staining appear normal (Fig. 7B, D). In normal mature vessels there is a positive correlation between arterial caliber and the thickness of the surrounding smooth muscle cell layer. Thus, an enlarged VSMC layer surrounding the dilated vessels might be anticipated. However, transversely sectioned vessels show no significant difference in the thickness of the smooth muscle alpha actin immunoreactive cell layer around the subclavian arteries of Smad7 virus-infected or control limbs (Fig. 7A–D). The lack of change might reflect either a specific effect of Smad7 misexpression, or the early developmental stage of the vasculature.

We also examined vascular smooth muscle cell distribution associated with the lateral midbrain vessels of Smad7 virus-infected heads (Fig. 4E, F). Whole mount immunostaining for smooth muscle alpha actin in normal embryos reveals that unlike in the limb, even small cranial capillaries possess a smooth muscle coating (Fig. 7E). Smad7 virus infection of developing brain ventricles at HH st15 causes dilation of the main vascular branches supplying blood to the midbrain within 48 h, as well as intra-arterial shunting and a reduction in the complexity of the secondary branching patterns (Figs. 4E, F; 7F). In these heads all vessels also possess an apparently normal smooth muscle coat (Fig. 7F).

Taken together these results suggest that the increase in vessel caliber caused by Smad7 misexpression is independent of VSMC recruitment, as we observe vessel dilation both in the absence and presence of VSMCs. In addition they indicate that VSMC recruitment, differentiation and maintenance are not blocked by Smad7 misexpression.

DISCUSSION

Our data demonstrate that Smad7 misexpression has profound effects on vascular development. We have used a replication competent retrovirus to misexpress Smad7 in the developing limb and head during periods of angiogenesis, subsequent to initial formation of the embryonic vasculature. We observe significant and rapid vessel dilation, but no loss of vessel integrity or alteration of the endothelial cell layer except for an increase in endothelial cell number commensurate with the changes in vessel size. Smad7 misexpression also causes inappropriate merging of vessels and gross vascular malformations, including arteriovenous and intravascular shunting. Interestingly Smad7 misexpression appears to only mildly delay angiogenic vessel branching. We observe no consistent correlation between vascular smooth muscle cells and the Smad7 vascular phenotype. The vascular phenotypes occur regardless of differentiated VSMC association with affected vessels, and VSMC recruitment, differentiation and maintenance are unaffected by Smad7 misexpression.

Signaling Pathways Influenced by Smad7 Misexpression

Our results raise several interesting questions about the identity of the signals, their signal transduction pathways, and the cellular targets upon which Smad7 might be acting. Smad7 can block signaling by BMP, activin, and TGFβ family ligands (Nakao *et al.*, 1997; Bhushan *et al.*, 1998; Casellas and Brivanlou, 1998; Ishisaki *et al.*, 1998; Ishisaki *et al.*, 1999; Massague, 1998). Multiple BMP family members are expressed in the developing limb and head, while both TGFβ and activin family members are expressed in association with the vasculature (Hogan, 1996; Matzuk *et al.*, 1995a,b; Pepper, 1997). Thus, Smad7 might be blocking signals from any of the major TGFβ superfamily protein families. However, the combination of our gene misexpression experiments and previously described gene knockout experiments suggest that some of these signals are less likely targets than others. Misexpression of neither noggin nor a dominant negative BMP receptor caused Smad7-like vascular phenotypes. They both caused other limb developmental defects that are consistent with previous reports, indicating that these reagents are active in our experiments (Capdevila and Johnson, 1998; Pizette and Niswander, 1999; Zou *et al.*, 1997). *In vitro* binding studies and *in vivo* misexpression studies indicate that noggin blocks a broad range of BMP family ligands, including BMP2, BMP4, and BMP7, the primary BMPs expressed in the developing limb and head (Capdevila and Johnson, 1998; Pizette and Niswander, 1999; Zimmerman *et al.*, 1996; A. Economides, Regeneron Corp, personal communication). While activins are expressed in the developing vasculature, activin null mice do not display vascular phenotypes (Matzuk *et al.*, 1995a,b). The ligand expression patterns combined with gene knockout and viral misexpression phenotypes suggest that the vascular Smad7 phenotype is not due to inhibition of BMP or activin signals.

Despite the noggin and BMPR Ib^{DN} data suggesting that BMP-type ligands are not vascular regulators, we observe that constitutive activation of BMP receptor intracellular signaling pathways is sufficient to inhibit the formation of Smad7-induced vascular defects. This result suggests that a non-BMP ligand (or ligands) acts through the intracellular side of the BMP pathway, perhaps through activation of a different receptor that impinges on the same signal transduction pathway. BMPR Ia and BMPR Ib activate the Smad1/Smad5/Smad8 cohort of positive Smad proteins, targets that are shared by an activated Alk1 receptor (Eppert *et al.*, 1996; Hoodless *et al.*, 1996; Massague and Chen, 2000; Oh *et al.*, 2000). However, the functional ligands for Alk1 are poorly defined; Alk1 can bind TGFβ protein, but has not been shown to be activated by it (Chen and Massague, 1999; Oh *et al.*, 2000). Intriguingly, loss of function Alk1 and Smad5 mutant mice have vascular phenotypes that are similar to, but distinct from, those we observe following Smad7 misexpression (Chang *et al.*, 1999; Oh *et al.*, 2000; Urness *et al.*, 2000; Yang *et al.*, 1999). Another possibility is that Smad7 is interfering with a non-TGFβ superfamily type signal, as Smad proteins can interact with non-TGFβ signaling pathways (Casellas and Brivanlou, 1998; Nagarajan *et al.*, 2000; Ulloa *et al.*, 1999). However, our activated BMP receptor rescue experiments strongly suggest that TGFβ superfamily signaling is the functional target.

TGFβ proteins are expressed in association with the developing vasculature and *in vitro* can have profound effects on endothelial cell and vascular smooth muscle cell growth and differentiation, as well as endothelial tube morphogenesis. TGFβ1 in particular is highly expressed by peripheral endothelial cells and is required for normal vascular development (Dickson *et al.*, 1995; Gatherer *et al.*, 1990; Pepper, 1997; Schmid *et al.*, 1991). Thus, TGFβ1, or another unknown but related ligand, or ligand heterodimer combination, perhaps acting through Alk1 and Smad5, is the most likely candidate for activating the pathway with which Smad7 is interfering.

The most likely cell type on which Smad7 is acting is the endothelial cells. They are the only cells definitively affected by Smad7 misexpression, increasing in number in association with changes in the vasculature. While Smad7 might affect vascular smooth muscle cells, we observe clear defects in vessels, such as the posterior marginal vein of the limb, that have no associated differentiated VSMCs. We also observe no obvious changes in the recruitment, differentiation or maintenance of the VSMC layer surrounding affected vessels in the limb or head. While we always observe infection of the vascular endothelium of dilated vessels, we can not rule out the possibility that nonvascular mesenchymal cells are affected, since the replication-competent RCAS virus infects these cells as well.

Normal Role of Smad7 as a Regulator of Vascular Caliber

Smad7 is a signaling antagonist that likely normally acts to attenuate positive TGFβ superfamily signals. By expressing Smad7 under the control of the RSV LTR of the RCAS virus, we have decoupled Smad7 expression from its normal transcriptional regulation. Therefore, the vascular phenotypes we observe can provide some insights into possible normal roles of Smad7 and TGFβ superfamily signals as regulators of vascular development.

Our studies suggest a dual role for endogenous Smad7. Endothelial Smad7 expression can be induced either by activation of the TGFβ superfamily signaling pathway, or by flow-induced shear stress, and endogenous Smad7 levels are higher in larger vessels during murine development (Topper *et al.*, 1997; Zwijsen *et al.*, 2000). Our experiments indicate that viral Smad7 causes vessel dilation throughout the noncapillary vasculature, presumably due to increased Smad7 levels, while constitutive activation of the BMP signaling pathway counteracts this effect. Thus, TGFβ

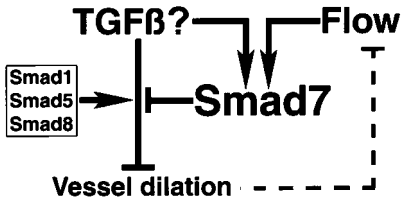

FIG. 8. Model of TGFβ regulation of vessel caliber. TGFβ signals received by endothelial cells and transduced via the positive Smads, Smad1, Smad5, and Smad8, reduce vessel caliber, while signal strength is attenuated by Smad7 through a negative feedback mechanism. Smad7 can also be independently induced via a flow-mediated mechanism, thus providing an additional reduction in TGFβ signal strength. If flow is reduced, vessels constrict, while if flow is increased, vessels dilate. These changes take place over a long time period relative to pharmacological constriction and dilation mediated by the vascular smooth muscle layer. TGFβ in the figure can be representative of any TGFβ superfamily ligand, although the TGFβ1 isoform seems most likely (see text).

superfamily signals acting through Smad1/Smad5/Smad8 might normally function to constrain vessel size, and compete with feedback-induced Smad7 to establish a steady-state vascular caliber (Fig. 8). Increased flow during embryonic growth might be responsible in part for the higher endogenous Smad7 levels in larger vessels, independent of TGFβ superfamily signals. This would shift the balance between TGFβ signaling and Smad7, and could in turn lead to increased vessel size, thus accommodating the larger circulatory needs of the growing embryo (Fig. 8).

While Smad7 virus-infected blood vessels contain up to threefold more endothelial cells, the source of these cells is unclear. The simplest explanation is that endothelial cell proliferation is increased, consistent with *in vitro* inhibition of endothelial cell growth by TGFβ (Pepper, 1997). However, in preliminary studies, we have not been able to detect significant changes in endothelial cell proliferation (data not shown). Alternatively, Smad7 might reduce TGFβ-mediated endothelial cell death, lead to the recruitment of additional endothelial cell precursors from the circulation, or promote transdifferentiation of surrounding mesenchymal cells (Pepper, 1997; Yamashita *et al.*, 2000). Other mechanisms by which vessel size might be increased are by suppressing secondary sprout formation, or by causing fusion of neighboring vessels. Consistent with this idea, excess vessel fusion has been reported in Alk1 null mice (Urness *et al.*, 2000). However, while we do detect increased avascular regions surrounding enlarged vessels (Figs. 1F, H; 4D, E), this is not always the case, especially in the midbrain near the dilated internal carotid arteries, where the surrounding vasculature looks essentially normal (Fig. 4A-C).

Function of Vascular Smooth Muscle Cells in Vascular Development

The relationship between vascular smooth muscle cells, TGFβ superfamily signals and vascular development is complex, and incompletely resolved. VSMCs are thought to interact with the vascular endothelium to maintain vascular integrity, and are also proposed to regulate vessel caliber by activating TGFβ signals to the underlying endothelium, thus inhibiting endothelial proliferation. Reciprocal TGFβ superfamily signals from the endothelial cells are thought to be required for recruitment, differentiation and/or maintenance of vascular smooth muscle cells during development and in adults (Folkman and D'Amore, 1996; Pepper, 1997; Yancopoulos *et al.*, 2000).

Our data indicate that neither vessel caliber nor integrity necessarily depends on vascular smooth muscle-endothelial interactions during development, despite their linkage in some germline mouse mutants (Chang *et al.*, 1999; Li *et al.*, 1999; Oh *et al.*, 2000; Puri *et al.*, 1995; Sato *et al.*, 1995; Suri *et al.*, 1996; Urness *et al.*, 2000; Vikkula *et al.*, 1996; Yang *et al.*, 1999). Following Smad7 virus infection we observe vascular dilation without any loss of structural integrity even in the absence of differentiated VSMCs, as seen, for example, in the posterior marginal vein of the limb. Once the vascular smooth muscle layer is formed, however, it might normally constrain vessel caliber through activation of latent TGFβ ligand (Folkman and D'Amore, 1996). If this is the case, Smad7 misexpression in our experiments would functionally uncouple these two cell types by preventing TGFβ signal transduction despite ligand activation, thereby allowing vessel dilation. However, as vascular integrity is not compromised in dilated vessels that retain a VSMC coat, then VSMC maintenance of vessel integrity and VSMC regulation of caliber apparently do not involve a common signaling system.

Smad7 viral misexpression also dissociates the processes of vascular smooth muscle cell recruitment, differentiation and maintenance from TGFβ superfamily signaling. During chick limb development, differentiated VSMCs, as identified by smooth muscle alpha actin immunoreactivity, are present initially surrounding only the proximal subclavian artery and are recruited to additional vessels over time. Smad7 misexpression does not affect either the maintenance of the VSMC coat, or the recruitment of VSMCs to more distal regions. Cranial vessels, which develop contemporaneously with their VSMC coat, have an apparently normal VSMC layer despite Smad7-induced dilation. Thus, Smad7 misexpression, and by inference, reduced TGFβ superfamily signaling, does not interfere with normal VSMC development.

Comparison with in Vivo Loss of Function Data

HHT patients, as well as endoglin, Alk1 and Smad5 null mutant mice, each of which is defective in TGFβ superfam-

ily signaling, have vascular phenotypes that are distinct from those observed following Smad7 misexpression (Chang *et al.*, 1999; Li *et al.*, 1999; Oh *et al.*, 2000; Shovlin and Letarte, 1999; Urness *et al.*, 2000; Yang *et al.*, 1999). In each mutant recruitment or maintenance of the vascular smooth muscle layer is disrupted and vascular integrity is significantly compromised, in striking contrast to the apparently normal vascular smooth muscle layer and intact vessels associated with Smad7 misexpression. Several explanations for these phenotypic differences are worth considering.

One possibility is that the signaling defect in the germline mutants might be qualitatively different from that caused by Smad7. The mutations in the endoglin, Alk1 and Smad5 genes might disrupt a critical balance between the parallel Smad2/Smad3 and Smad1/Smad5/Smad8 branches of the TGFβ superfamily signaling pathway (Oh *et al.*, 2000). In contrast Smad7, a broad spectrum signal transduction antagonist, might interfere with each branch to a similar degree. Gross pathway imbalance in the mutants might thus lead to more severe outcomes than an overall signal blockade. While a distinct possibility, our results demonstrating that activation of only the BMP receptor side of the pathway is sufficient to prevent the Smad7-induced vascular phenotype strongly suggests that balanced pathway activation is not critical.

Mice lacking Alk1, endoglin or Smad5 function die during early angiogenesis, as they suffer from a general disruption of cardiovascular function (Chang *et al.*, 1999; Li *et al.*, 1999; Oh *et al.*, 2000; Urness *et al.*, 2000; Yang *et al.*, 1999). Impaired VSMC recruitment or reduced vascular integrity in these animals might be secondary to a developmental delay, or the decline in overall embryonic health. Alternatively, the more severe germline phenotypes might result from earlier, hidden vasculogenic defects that are unmasked as development proceeds. Because Smad7 virus infection is localized within the embryo, and occurs after establishment of the primary circulation, such secondary effects might not be observed.

Implications for Etiology of Arterio-Venous Malformations (AVM)

We observed arterio-venous shunts in the vasculature of the majority of Smad7 virus-infected limbs. These results are consistent with previous reports that link the TGFβ superfamily pathway to arterio-venous malformations, and suggest that Smad7 misexpression is a useful model for studying AVM formation. In human patients AVMs are clinically significant vascular structures. Shunting blood directly between the arterial and venous circulations can make more distal structures hypoxic, and can disrupt critical capillary-based functions in organs such as the lungs or liver (Shovlin and Letarte, 1999). In addition increased blood volume combined with the loss of vascular resistance to flow can lead to heart failure (Shovlin and Letarte, 1999). Both Smad7 gain of function and germline Alk1 loss of function can cause AVM formation, however these models differ as the Smad7-induced AVMs form substantially after the onset of angiogenesis.

AVMs are characterized by anomolous arterio-venous connections and dilated vessels feeding into and out of the shunt. These phenotypes might arise independently, or via a temporally linked mechanism. In Alk1 null mutant mice shunt formation is the earliest visible vascular defect, occurring prior to vessel dilation (Urness *et al.*, 2000). In contrast in HHT patients, arteriole and venule dilation is observed in hemorrhagic vascular beds; whether these malformations progress into distinct AVMs has not been determined (Shovlin and Letarte, 1999). Our data demonstrate that Smad7-induced arterial and venous vessel dilation can precede shunt formation, and that shunt formation is not an inevitable secondary consequence of vessel dilation, at least for the duration of these experiments. Taken together, these data suggest that shunt formation and vessel dilation can be independent consequences of defects in TGFβ signaling.

Analysis of endothelial cells of Alk1 null mutants suggests that arterial/venous identity of noncapillary vessels is never established (Urness *et al.*, 2000). This phenotype is thought to result, at least in part, from impaired Eph/Ephrin signaling at the earliest stages of angiogenesis, thus leading to a lack of mutual repulsion between arterial and venous endothelial sprouts (Urness *et al.*, 2000). It will be interesting to determine whether similar mechanisms are implicated in causing the Smad7-induced AVMs. These AVMs all form from established vessels, and Smad7 misexpression would thus have to repress pre-existing arterial and venous identities, rather than inhibit their establishment. Shunting in the cranial vasculature occurs within an individual vessel (Fig. 4C); or between the right and left internal carotid arteries (Fig. 4B). Thus, either distinct TGFβ signaling-dependent mechanisms cause arterial and arterio-venous malformations, or a lack of arterio-venous distinctions is not the only contributory factor in AVM formation.

ACKNOWLEDGMENTS

We are very grateful to Rich Blazeski for his time and expert help with the transmission electron microscopy; and Artur Kania for his help and advice with confocal microscopy; Lynda Erskine, Luisa Iruela-Arispe, Nick Gale, Tom Jessell, Claire Shovlin, Claudio Stern, Cliff Tabin, and Gavin Thurston for critical reading of the manuscript and helpful suggestions. We also thank John Fallon, Katherine Galvin and Charles Little for stimulating discussions, and Jan Christian for providing the xSmad7 cDNA. We are grateful to members of the Laufer and Stern Labs for helpful comments and suggestions throughout the course of this work.

N. V. was supported by a fellowship from the Human Frontiers Science Program. This work was supported by grants from the American Cancer Society (ACS-IRG-88-006-10), and the Irma T. Hirschl/Monique Weill-Caulier Trust to E. L., and funds from the HHMI Research Resources Program for Medical Schools.

REFERENCES

Afrakhte, M., Moren, A., Jossan, S., Itoh, S., Sampath, K., Westermark, B., Heldin, C. H., Heldin, N. E., and ten Dijke, P. (1998). Induction of inhibitory Smad6 and Smad7 mRNA by TGF-beta family members. *Biochem. Biophys. Res. Commun.* **249,** 505–511.

Ambler, C. A., Nowicki, J. L., Burke, A. C., and Bautch, V. L. (2001). Assembly of trunk and limb blood vessels involves extensive migration and vasculogenesis of somite-derived angioblasts. *Dev. Biol.* **234,** 352–364.

Bhushan, A., Chen, Y., and Vale, W. (1998). Smad7 inhibits mesoderm formation and promotes neural cell fate in Xenopus embryos. *Dev. Biol.* **200,** 260–268.

Brand-Saberi, B., Seifert, R., Grim, M., Wilting, J., Kuhlewein, M., and Christ, B. (1995). Blood vessel formation in the avian limb bud involves angioblastic and angiotrophic growth. *Dev. Dyn.* **202,** 181–194.

Capdevila, J., and Johnson, R. L. (1998). Endogenous and ectopic expression of noggin suggests a conserved mechanism for regulation of BMP function during limb and somite patterning. *Dev. Biol.* **197,** 205–217.

Casellas, R., and Brivanlou, A. H. (1998). Xenopus Smad7 inhibits both the activin and BMP pathways and acts as a neural inducer. *Dev. Biol.* **198,** 1–12.

Chang, H., Huylebroeck, D., Verschueren, K., Guo, Q., Matzuk, M., and Zwijsen, A. (1999). Smad5 knockout mice die at midgestation due to multiple embryonic and extraembryonic defects. *Development* **126,** 1631–1642.

Chen, Y. G., and Massague, J. (1999). Smad1 recognition and activation by the ALK1 group of transforming growth factor-beta family receptors. *J. Biol. Chem.* **274,** 3672–3677.

Christian, J. L., and Nakayama, T. (1999). Can't get no SMADisfaction: Smad proteins as positive and negative regulators of TGF-beta family signals. *Bioessays* **21,** 382–390.

Coffin, J. D., and Poole, T. J. (1988). Embryonic vascular development: immunohistochemical identification of the origin and subsequent morphogenesis of the major vessel primordia in quail embryos. *Development* **102,** 735–748.

Daniel, T. O., and Abrahamson, D. (2000). Endothelial signal integration in vascular assembly. *Annu. Rev. Physiol.* **62,** 649–671.

Dickson, M. C., Martin, J. S., Cousins, F. M., Kulkarni, A. B., Karlsson, S., and Akhurst, R. J. (1995). Defective hematopoiesis and vasculogenesis in transforming growth factor-beta 1 knock out mice. *Development* **121,** 1845–1854.

Ebisawa, T., Fukuchi, M. Murakami, G., Chiba, T., Tanaka, K., Imamura, T., and Miyaono, K. (2001). Smurf1 interacts with Transforming Growth Factor-β Type I receptor through Smad7 and induces receptor degradation. *J. Biol. Chem.* **276,** 12477–12480.

Eppert, K., Scherer, S. W., Ozcelik, H., Pirone, R., Hoodless, P., Kim, H., Tsui, L. C., Bapat, B., Gallinger, S., Andrulis, I. L., Thomsen, G. H., Wrana, J. L., and Attisano, L. (1996). MADR2 maps to 18q21 and encodes a TGFbeta-regulated MAD-related protein that is functionally mutated in colorectal carcinoma. *Cell* **86,** 543–52.

Fallon, J. F., and Kelley, R. O. (1977). Ultrastructural analysis of the apical ectodermal ridge during vertebrate limb morphogenesis. II. Gap junctions as distinctive ridge structures common to birds and mammals. *J. Embryol. Exp. Morphol.* **41,** 223–232.

Folkman, J., and D'Amore, P. A. (1996). Blood vessel formation: What is its molecular basis? *Cell* **87,** 1153–1155.

Gajdusek, C. M., Luo, Z., and Mayberg, M. R. (1993). Basic fibroblast growth factor and transforming growth factor beta-1: Synergistic mediators of angiogenesis in vitro. *J. Cell. Physiol.* **157,** 133–144.

Gale, N. W., and Yancopoulos, G. D. (1999). Growth factors acting via endothelial cell-specific receptor tyrosine kinases: VEGFs, angiopoietins, and ephrins in vascular development. *Genes. Dev.* **13,** 1055–1066.

Gatherer, D., ten Dijke, P., Baird, D. T., and Akhurst, R. J. (1990). Expression of TGF-beta isoforms during first trimester human embryogenesis. *Development* **110,** 445–460.

Hamburger, V., and Hamilton, H. L. (1951). A series of normal stages in the development of the chick embryo. *J. Exp. Morph.* **88,** 49–92.

Hayashi, K., Ishidou, Y., Yonemori, K., Nagamine, T., Origuchi, N., Maeda, S., Imamura, T., Kato, M., Yoshida, H., Sampath, T. K., ten Dijke, P., and Sakou, T. (1997). Expression and localization of bone morphogenetic proteins (BMPs) and BMP receptors in ossification of the ligamentum flavum. *Bone* **21,** 23–30.

Hogan, B. L. (1996). Bone morphogenetic proteins in development. *Curr. Opin. Genet. Dev.* **6,** 432–438.

Hoodless, P. A., Haerry, T., Abdollah, S., Stapleton, M., O'Connor, M. B., Attisano, L., and Wrana, J. L. (1996). MADR1, a MAD-related protein that functions in BMP2 signaling pathways. *Cell* **85,** 489–500.

Hughes, A. (1934). On the development of the blood vessels in the head of the chick. *Phil. Trans. Roy. Soc. Ser. B* **224,** 75–130.

Hungerford, J. E., and Little, C. D. (1999). Developmental biology of the vascular smooth muscle cell: building a multilayered vessel wall. *J. Vasc. Res.* **36,** 2–27.

Ishisaki, A., Yamato, K., Nakao, A., Nonaka, K., hguchi, M., ten Djke, P., and Nishihara, T. (1998). Smad7 is a Activin-inducible inhibitor of Activin-induced growth arrest and apoptosis in mouse B cells. *J. Biol. Chem.* **273,** 24293–24296.

Ishisaki, A., Yamato, K., Hashimoto, S., Nakao, A., Tamaki, K., Nonaka, K., ten Dijke, P., Sugino, H., and Nishihara, T. (1999). Differential inhibition of Smad6 and Smad7 on Bone Morphogenetic Protein- and Activin-mediated growth arrest and apoptosis in B cells. *J. Biol. Chem.* **274,** 13637–13642.

Itoh, S., Landstrom M., Hermansson, A., Itoh, F., Heldin, C-H., Heldin, N-E., and ten Dijke, P. (1998). Transforming Growth Factor β1 induces nuclear export of inhibitory Smad7. *J. Biol. Chem.* **273,** 29195–29201.

Kardon, G. (1998). Muscle and tendon morphogenesis in the avian hind limb. *Development* **125,** 4019–4032.

Kavsak, P., Rasmussen, R. K., Causing, C. G., Bonni, S., Zhu, H., Thomsen, G. H., and Wrana, J. L (2000). Smad7 binds to Smurf2 to form an E3 ubiquitin ligase that targets the TGFβ receptor for degradation. *Molecular Cell* **6,** 1365–1375.

Klagsbrun, M., and D'Amore, P. A. (1991). Regulators of angiogenesis. *Annu. Rev. Physiol.* **53,** 217–239.

Lawler, J., Sunday, M., Thibert, V., Duquette, M., George, E. L., Rayburn, H., and Hynes, R. O. (1998). Thrombospondin-1 is required for normal murine pulmonary homeostasis and its absence causes pneumonia. *J. Clin. Invest.* **101,** 982–992.

Li, D. Y., Sorenson, L. K., Brooke, B. S., Urness L. D., Davis, E. C., Taylor, D. G., Boak, B. B., and Wendel, D. P. (1999). Defective angiogenesis in mice lacking Endoglin. *Science* **284,** 1534–1537.

Logan, M., Pagan-Westphal, S. M., Smith, D. M., Paganessi, L., and Tabin, C. J. (1998). The transcription factor Pitx2 mediates situs-specific morphogenesis in response to left-right asymmetric signals. *Cell* **94,** 307–317.

Logan, M., and Tabin, C. (1998). Targeted gene misexpression in chick limb buds using avian replication-competent retroviruses. *Methods* **14,** 407–420.

Madri, J. A., Pratt, B., and Tucker, A. M. (1988). Phenotypic modulation of endothelial cells by transforming growth factor-β depends on the composition and organization of the extracellular matrix. *J Cell Biol* **106,** 1357–1384.

Massague, J. (1998). TGF-beta signal transduction. *Annu. Rev. Biochem.* **67,** 753–791.

Massague, J., and Chen, Y. G. (2000). Controlling TGF-beta signaling. *Genes Dev.* **14**, 627–644.

Matzuk, M. M., Kumar, T. R., and Bradley, A. (1995a). Different phenotypes for mice deficient in either activins or activin receptor type II. *Nature* **374**, 356–360.

Matzuk, M. M., Kumar, T. R., Vassalli, A., Bickenbach, J. R., Roop, D. R., Jaenisch, R., and Bradley, A. (1995b). Functional analysis of activins during mammalian development. *Nature* **374,** 354–6.

Merwin, J. R., Anderson, J. M., Kocher, O., van Itallie, C., Madri, J. (1990). Transforming growth factor-β1 modulates extracellular matrix organization and cell-cell junctional complex formation during in vitro angiogenesis. *J. Cell Physiol.* **142,** 117–128.

Miyazono, K. (2000). TGF-beta signaling by Smad proteins. *Cytokine Growth Factor Rev.* **11,** 15–22.

Nagarajan, R. P., Chen, F., Li, W., Vig, E., Harrington, M. A., Nakshatri, H., and Chen Y. (2000). Repression of transforming-growth-factor-beta-mediated transcription by nuclear factor kappaB. *Biochem. J.* **348,** 591–596.

Nakao, A., Afrakhte, M., Moren, A., Nakayama, T., Christian, J. L., Heuchel, R., Itoh, S., Kawabata, M., Heldin, N-E., Heldin, C-H., and ten Dijke, P. (1997). Identification of Smad7, a TGFβ-inducible anatagonist of TGF-β signaling. *Nature* **389,** 631–635.

Nakayama, T., Gardner, H., Berg, L. K., and Christian, J. L. (1998a). Smad6 functions as an intracellular antagonist of some TGF-beta family members during Xenopus embryogenesis. *Genes Cells* **3,** 387–394.

Nakayama, T., Snyder, M. A., Grewal, S. S., Tsuneizumi, K., Tabata, T., and Christian, J. L. (1998b). Xenopus Smad8 acts downstream of BMP-4 to modulate its activity during vertebrate embryonic patterning. *Development* **125,** 857–867.

Nakayama, T., Berg, L. K., and Christian, J. L. (2001). Dissection of inhibitory Smad proteins: both N- and C-terminal domains are necessary for full activities of Xenopus Smad6 and Smad7. *Mech. Dev.* **100,** 251–262.

Oh, S. P., Seki, T., Goss, K. A., Imamura, T., Yi, Y., Donahoe, P., Li, L., Miyazono, K., ten Dijke, P., Kim, S., and Li, E. (2000). Activin receptor-like kinase 1 modulates transforming growth factor-beta1 signaling in the regulation of angiogenesis. *Proc. Natl. Acad. Sci. USA* **97,** 2626–2631.

Oshima, M., Oshima, H., and Taketo, M. M. (1996). TGF-beta receptor type II deficiency results in defects of yolk sac hematopoiesis and vasculogenesis. *Dev. Biol.* **179,** 297–302.

Pardanaud, L., Altmann, C., Kitos, P., Dieterlen-Lievre, F., and Buck, C. A. (1987). Vasculogenesis in the early quail blastodisc as studied with a monoclonal antibody recognizing endothelial cells. *Development* **100,** 339–349.

Pardanaud, L., Yassine, F., and Dieterlen-Lievre, F. (1989). Relationship between vasculogenesis, angiogenesis and hemopoiesis during avian ontogeny. *Development* **105,** 473–485.

Pelton, R. W., Nomura, S., Moses, H. L., and Hogan, B. L. (1989). Expression of transforming growth factor beta 2 RNA during murine embryogenesis. *Development* **106,** 759–767.

Pelton, R. W., Dickinson, M. E., Moses, H. L., and Hogan, B. L. (1990). In situ hybridization analysis of TGF beta 3 RNA expression during mouse development: comparative studies with TGF beta 1 and beta 2. *Development* **110,** 609–620.

Pepper, M. S. (1997). Transforming growth factor-beta: Vasculogenesis, angiogenesis, and vessel wall integrity. *Cytokine Growth Factor Rev.* **8,** 21–43.

Pepper, M. S., Belin, D., Montesano, R., Orci, L., and Vassalli, J-D. (1990). Transforming growth factor beta-I modulates basic-fibroblast growth factor-induced proteolytic and angiogenic properties of endothelial cells in vitro. *J. Cell Biol.* **11,** 743–755.

Pepper, M. S., Vassalli, J-D., Orci, L., and Montesan, R. (1993). Biphasic effect of transforming growth factor-beta I on in vitro angiogenesis. *Exp. Cell Res.* **204,** 356–363.

Pizette, S., and Niswander, L. (1999). BMPs negatively regulate structure and function of the limb apical ectodermal ridge. *Development* **126,** 883–894.

Poole, T. J., and Coffin, J. D. (1989). Vasculogenesis and angiogenesis: two distinct morphogenetic mechanisms establish embryonic vascular pattern. *J. Exp. Zool.* **251,** 224–231.

Potts, W. M., Olsen, M., Boettiger, D., and Vogt, V. M. (1987). Epitope mapping of monoclonal antibodies to gag protein p19 of avian sarcoma and leukaemia viruses. *J. Gen. Virol.* **68,** 3177–3182.

Puri, M. C., Rossant, J., Alitalo, K., Bernstein, A., and Partanen, J. (1995). The receptor tyrosine kinase TIE is required for integrity and survival of vascular endothelial cells. *EMBO J.* **14,** 5884–5891.

Riddle, R. D., Johnson, R. L., Laufer, E., Tabin, C. (1993). Sonic hedgehog mediates the polarizing activity of the ZPA. *Cell* **75,** 1401–1416.

Risau, W. (1997). Mechanisms of angiogenesis. *Nature* **386,** 671–674.

Roberts, A. B., and Sporn, M. B. (1989). Regulation of endothelial cell growth, architecture, and matrix synthesis by TGF-beta. *Am. Rev. Respir. Dis.* **140,** 1126–1128.

Roberts, A. B., and Sporn, M. B. (1992). Differential expression of the TGF-beta isoforms in embryogenesis suggests specific roles in developing and adult tissues. *Mol. Reprod. Dev.* **32,** 91–98.

Sato, T. N., Tozawa, Y., Deutsch, U., Wolburg-Buchholz, K., Fujiwara, Y., Gendron-Maguire, M., Gridley, T., Wolburg, H., Risau, W., and Qin, Y. (1995). Distinct roles of the receptor tyrosine kinases Tie1 and Tie2 in blood vessel formation. *Nature* **376,** 70–74.

Schmid, P., Cox, D., Bilbe, G., Maier, R., and McMaster, G. K. (1991). Differential expression of TGF beta 1, beta 2 and beta 3 genes during mouse embryogenesis. *Development* **111,** 117–130.

Shovlin, C. L., and Letarte, M. (1999). Hereditary hemorrhagic telangiectasia and pulmonary arteriovenous malformations: issues in clinical management and review of pathogenic mechanisms. *Thorax* **54,** 714–729.

Souchelnytskyi, S., Nakayama, T., Nakao, A., Moren, A., Heldin, C. H., Christian, J. L., and ten Dijke, P. (1998). Physical and functional interaction of murine and Xenopus Smad7 with bone

morphogenetic protein receptors and transforming growth factor-beta receptors. *J. Biol. Chem*. **273,** 25364–25370.

Suri, C., Jones, P. F., Patan, S., Bartunkova, S., Maisonpierre, P. C., Davis, S., Sato, T. N., and Yancopoulos, G. D. (1996). Requisite role of angiopoietin-1, a ligand for the TIE2 receptor, during embryonic angiogenesis. *Cell* **87,** 1171–1180.

Thurston, G., Baluk, P., Hirata, A., and McDonald, D. M. (1996). Permeability-related changes revealed at endothelial cell borders in inflamed venules by lectin binding. *Am. J. Physiol.* **271,** H2547–2562.

Topper, J. N., Cai, J., Qiu, Y., Anderson, K. R., Xu, Y. Y., Deeds, J. D., Feeley, R., Gimeno, C. J., Woolf, E. A., Tayber, O., et al. (1997). Vascular MADs: Two novel MAD-related genes selectively inducible by flow in human vascular endothelium. *Proc. Natl. Acad. Sci. USA* **94,** 9314–9319.

Tsuneizumi, K., Nakayama, T., Kamoshida, Y., Kornberg, T. B., Christian, J. L., and Tabata, T. (1997). Daughters against dpp modulates dpp organizing activity in Drosophila wing development. *Nature* **389,** 627–631.

Ulloa, L., Doody, J., and Massague, J. (1999). Inhibition of transforming growth factor-beta/SMAD signalling by the interferon-gamma/STAT pathway. *Nature* **397,** 710–713.

Urness, L. D., Sorensen, L. K., and Li, D. Y. (2000). Arteriovenous malformations in mice lacking activin receptor-like kinase-1. *Nat. Genet.* **26,** 328–331.

Vikkula, M., Boon, L. M., Carraway, K. L., Calvert, J. T., Diamonti, A. J., Goumnerov, B., Pasyk, K. A., Marchuk, D. A., Warman, M. L., Cantley, L. C., Mulliken, J. B., and Olsen, B. R. (1996). Vascular dysmorphogenesis caused by an activating mutation in the receptor tyrosine kinase TIE2. *Cell* **87,** 1181–1190.

Yamashita, J., Itoh, H., Hirashima, M., Ogawa, M., Nishikawa, S., Yurugi, T., Naito, M., and Nakao, K. (2000). Flk1-positive cells derived from embryonic stem cells serve as vascular progenitors. *Nature* **408,** 92–96.

Yancopoulos, G. D., Davis, S., Gale, N. W., Rudge, J. S., Wiegand, S. J., and Holash, J. (2000). Vascular-specific growth factors and blood vessel formation. *Nature* **407,** 242–248.

Yang, X., Castilla, L. H., Xu, X., Li, C., Gotay, J., Weinstein, M., Liu, P. P., Deng, C-X. (1999). Angiogenesis defects and mesenchymal apoptosis in mice lacking SMAD5. *Development* **126,** 1571–1580.

Zimmerman, L. B., De Jesus-Escobar, J. M., and Harland, R. M. (1996). The Spemann organizer signal noggin binds and inactivates bone morphogenetic protein 4. *Cell* **86,** 599–606.

Zou, H., Wieser, R., Massague, J., and Niswander, L. (1997). Distinct roles of type I bone morphogenetic protein receptors in the formation and differentiation of cartilage. *Genes Dev.* **11,** 2191–2203.

Zwijsen, A., van Rooijen, M. A., Goumans, M. J., Dewulf, N., Bosman, E. A., ten Dijke, P., Mummery, C. L., and Huylebroeck, D. (2000). Expression of the inhibitory Smad7 in early mouse development and upregulation during embryonic vasculogenesis. *Dev. Dyn.* **218,** 663–670.

Received for publication June 25, 2001
Revised October 3, 2001
Accepted October 3, 2001
Published online November 14, 2001